Journal of Renewable Materials

Tech Science Press

DOI: 10.32604/jrm.2022.019721

ARTICLE

Silk Fibroin-Based Hydrogel for Multifunctional Wearable Sensors

Yiming Zhao[1,2], Hongsheng Zhao[3], Zhili Wei[4], Jie Yuan[1], Jie Jian[1], Fankai Kong[1], Haojiang Xie[1] and Xingliang Xiong[1,2,*]

[1]College of Medical Informatics, Chongqing Medical University, Chongqing, 400016, China

[2]Medical Data Science Academy, Chongqing Medical University, Chongqing, 400016, China

[3]Communication and Information Center of Ministry of Emergency Management, Beijing, 100013, China

[4]The Ministry of Education Key Laboratory of Laboratory Medical Diagnostics, The College of Laboratory Medicine, Chongqing Medical University, Chongqing, 400016, China

[*]Corresponding Author: Xingliang Xiong. Email: xlxiong@cqmu.edu.cn

Received: 11 October 2021 Accepted: 05 November 2021

ABSTRACT

The flexible wearable sensors with excellent stretchability, high sensitivity and good biocompatibility are significantly required for continuously physical condition tracking in health management and rehabilitation monitoring. Herein, we present a high-performance wearable sensor. The sensor is prepared with nanocomposite hydrogel by using silk fibroin (SF), polyacrylamide (PAM), polydopamine (PDA) and graphene oxide (GO). It can be used to monitor body motions (including large-scale and small-scale motions) as well as human electrophysiological (ECG) signals with high sensitivity, wide sensing range, and fast response time. Therefore, the proposed sensor is promising in the fields of rehabilitation, motion monitoring and disease diagnosis.

KEYWORDS

Acrylic amide; silk fibroin; graphene oxide; wearable sensor; flexible strain sensor

1 Introduction

In recent years, the emergence of flexible sensors has greatly improved the comfort of the wear and the convenience of use compared to the traditional metal-based wearable sensor, which means they are more beneficial for long-term, continuous, and accurate monitoring of limb movement information in rehabilitation patients and physiological parameters in chronic patients. The flexible strain sensors [1,2] have attracted the most attention due to they can easily convert human movement deformation or physiological information into electrical signals (resistance or capacitance) by using a variety of conductive materials. In practical applications, the conductive materials (such as graphene [3], Multi-walled carbon nanotubes (MWCNTs), and MXene [4,5], etc.) were usually coated or deposited on the surface of polymer substrates (such as PDMS, PU, etc.). However, these methods will cause delamination between the conductive layer and elastic substrate in sensors due to the weak binding force of different materials, which will seriously affect the stability and service life of sensors [6,7]. In addition, the conductive composites based aerogel or hydrogel using intrinsically conductive polymers such as polyacetylene [8], polythiophene [9,10], polypyrrole (PPy) [11,12] have been widely studied in past

decade. It should be noted that these materials have several disadvantages, including poor elongation properties and complex preparation method. Moreover, these materials have poor self-adhesion and mechanical properties, which cannot meet the needs of practical application. Therefore, it is still an urgent problem [13–15] to prepare a flexible wearable device to meet the requirements of excellent sensitivity, good stability, and superior biocompatibility [16,17].

The hydrogels reveal a broad application prospect owing to their special mechanical properties similar to the skin tissues resulting to blur the boundary between wearable sensors and human skin. The conductive hydrogels prepared by mixing conductive nanomaterials (metal nanoparticles and graphene sheets) in polymers can greatly endow the hydrogel-based sensor with excellent electrical and mechanical properties [18–20]. Liao et al. used functionalized single-walled carbon nanotubes to prepare a nanocomposite hydrogel with good conductive and self-adhesive [21]. Annabi et al. proposed a graphene-based nanocomposite hydrogel with excellent sensing properties and good biocompatibility [22]. In addition, the polymer PAM which possesses good biocompatibility and mechanical tunability, has been widely used in the preparation of flexible wearable sensors. However, the pure PAM-based hydrogels have poor mechanical properties cannot be applied to flexible wearable devices alone [23,24]. Silk fibroin (SF) [25,26] is a natural protein that is widely used for its excellent mechanical toughness, ease of access, and good biocompatibility. Therefore, if the hydrogels prepared with both PAM and SF will have superior mechanical properties that can meet the requirements of wearable sensors for mechanical properties, elongation, and wear resistance [23,27,28].

In addition, the issue of conformal contact between the human skins and the surfaces of sensors is also not fully resolved [29,30], therefore, the difference of tensile and bending stiffness between human skin and sensor may seriously affect the measurement results, even if the sensor is attached to human skin by physical methods, such as adhesive bandages. The PDA molecules which possess similar structure to mussel adhesion protein, can firmly adhere to a wide variety of surfaces. Furthermore, the GO molecules can be reduced to the partly reduce graphene oxide (prGO) molecules by the DA molecules during the self-polymerization of the DA molecules to form PDA molecules [9,31]. Meanwhile, the PDA can also promote the dispersion of prGO in solution, thus facilitating the construction of a uniform prGO-based conductive network in hydrogel system [32,33].

In this work, a flexible wearable sensor was prepared by using GO, natural materials SF, eupolymer PAM and PDA. The hydrogel based sensor exhibits excellent electrical and mechanical properties, its conductivity, tensile stress, and tensile strain reach 10.5 mS cm^{-1}, 60.5 KPa and 1020%, respectively. Moreover, it shows excellent adhesion properties, which enable it to adhere to almost all types of organic and inorganic surfaces, such as glasses, human skins, and rubbers. In addition, due to the strong durability and repeatability of this hydrogel, it can be used on the human body directly to detect small-scale motions (the movement of the face, wrists, fists) and large-scale motions (the movement of the necks, knees, fingers). Furthermore, excellent biocompatibility is another property of hydrogels, ensuring the hydrogel can be used as electrodes to detect ECG signals without causing human skin reactions.

2 Experiment Section

2.1 Materials

SF was obtained from Southwest University., GO was purchased from Nanjing Jicang Nanotechnology Co., Ltd. (Nanjing, China) Acrylamide (Am), ammonium persulfate (APS), N, N′-Methylenebis(acrylamide) (MBA) and N, N, N′, N′-tetramethyl ethylenediamine(TEMED) were obtained from Aladdin. SF powder was obtained from China Tiansi Bio-Tech. DA was provided by BBI Co. (Shanghai, China), NIH_3T_3 cells obtained from our laboratory., Cell Counting Kit-8 (CCK-8) and Fetal Bovine Serum were obtained from Solarbio Life Science Co., Ltd (Beijing, China). Trypsin was purchased from Thermo Fisher Scientific. All the solvents in this work were analytical grades.

2.2 Preparation of SF Solution

(1) LiBr method: The cocoon pieces were boiled in 0.02 M/L Na_2CO_3 aqueous solution for 1 h. Then, wash the SF and place it in an oven at 50°C until dry thoroughly. After that, the dried SF was added to 9.3 M LiBr in a water bath at 60°C until it was completely dissolved. Dialysis the above solution for three days and change water every 12 h. Impurities were removed by centrifuging the solution, and then the obtained solution was stored at 4°C.

(2) Ternary solvent method: The solvent was prepared by the molar ratio of calcium chloride: ethanol: water = 1:2:8. Then put the degummed SF (Degumming steps are shown in (1)) in the ternary solvent in the water bath at 70°C for 4 h. The dialysis process is the same as (1).

2.3 Preparation of Hydrogels

(1) GO was dissolved in deionized water and ultrasonic dispersion. Then NaOH was used to adjust the pH value of GO solution to 11 and add DA to the above solution. Keep stirring at 70°C for 2 h at a speed of 500 rpm, then PAM and SF were added into the solution, and kept stirring until evenly dispersed.

(2) Formation of PAM-SF-PDA-prGO(PSPp) hydrogel: The MBA and APS were added into the (1) solution, then keep stirring for 10 min. Finally, TMEDA was added quickly and stirred until the hydrogel was formed and assembled as the flexible wearable sensor.

2.4 Characterization

The morphological characteristics and internal features of hydrogel were observed by SEM (Cai Si Gemini 300) and FTIR spectroscopy (Thermo IS50), respectively. Cell morphology was observed by Leica DMi8 inverted fluorescence microscope.

2.5 Mechanical Test

The hydrogels were cut into lengths, width, and thickness of 30, 10, and 3 mm respectively. These samples are used in tensile, antifatigue, and adhesion tests by the universal testing machine (E43, MTS). In this experiment, the moving speed of the tension machine is 40, 30, and 2 mm min^{-1}, respectively.

2.6 Electricity Test

Electrochemical workstations (CHI604E) were used to test the sensitivity and resistivity of hydrogels via the three-electrode double probe method. The hydrogel sensor and an electrochemical workstation are used to form a loop. Then, the sensor was placed on the finger, wrist, neck, throat, face, and knees of the human body to monitor electrical signals produced by different movements.

2.7 Swelling Test

The hydrogels (PAM, PS, PSP, PSPp) were dried to constant weight (W_0) by freeze-drying. The dried hydrogel was soaked in PBS solution, and the PBS on the surface was removed at the corresponding time and the swelling equilibrium mass (W_a) was measured. The swelling ratio (SR) of hydrogels is determined by the equation ($SR = (W_a - W_0)/W_0) \times 100\%$).

2.8 Cytotoxicity Evaluation

The cytotoxicity of hydrogel was evaluated by the CCK8 method using NIH3T3 fibroblasts. In the experimental group, PSPp hydrogel soaking solution was used as the culture medium. In addition, the culture medium was used as the negative control group. CCK8 detection reagent was added to the above two groups, and then cultured in cell incubator for 2 h. Then record the optical density (OD) detected by the microplate reader at 450 nm was used to calculate the biocompatibility of the hydrogel.

3 Results and Discussion

Fig. 1 illustrates the schematic of graphene-based, scalable, self-adhered, conductive hydrogel [34]. After DA was added to the alkaline solution, it will undergo a self-healing reaction immediately, with the increasing time of the self-polymerization reaction, the solution gradually changes from brown-yellow to black. During this process, the oxygen-containing functional groups of GO were reduced. Meanwhile, the generated PDA provides various non-covalent bonds that promote the dispersion of reduced graphene oxide(rGO) in water, which endows hydrogels with excellent conductivity. In addition, after PAM, SF, and crosslink agents were added to the solution, the functional groups of GO/rGO formed hydrogen bonds with amide groups in the PAM network (Fig. 1c). Therefore, it can be considered that strong hydrogen bonds connect PAM, SF, PDA, and GO into networks. Meanwhile, under the interaction of Vander Waals forces and covalent bond, the hydrogel exhibit outstanding tensile property and conductivity (Fig. 1c).

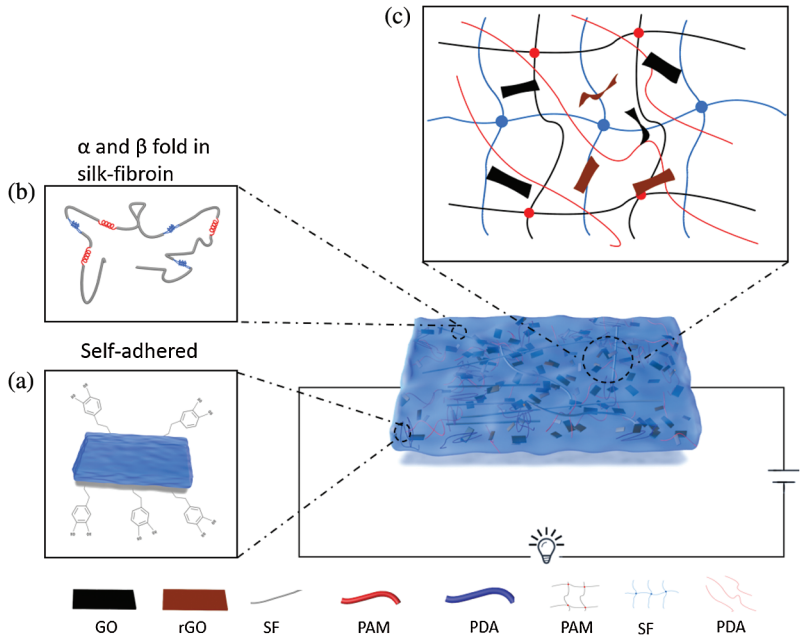

Figure 1: Schematic illustration of internal structure of PAM-SF-PDA-prGO (PSPp) hydrogel; (a) The residual catechol group of PDA chains endowed the PSPp hydrogel with self-adhersion property; (b) α and β folds in SF chains enhance the mechanical properties of hydrogels; (c) Schematic diagram of the PSPp hydrogel internal network

The fabrication procedures of the PSPp hydrogel are exhibited in Fig. 2. Firstly, DA was added to the GO dispersion and adjusted to pH 11 with NaOH, then the above solutions were mixed via a simple mixing method. Finally, PAM and corresponding crosslinker were added in order to form PSPp hydrogel interpenetrating network (the experimental part of the specific steps). In addition, to detect the signal of human motion, the PSPp hydrogel was connected with the electrochemical workstation to form a loop [35].

The cross-sectional structure of different components hydrogel sample was observed by SEM (Fig. 3). The porous structure of hydrogel can be observed, and the internal structure of the PAM hydrogel is porous and uniform. After introducing SF, the PS hydrogel exhibited clear and continuous uniform network structures, the pore wall structure is obviously changed and formed filament, as well as the pore size, is uneven and rough, implying that SF endows the hydrogel with excellent adhesion. In addition, the PSPp hydrogel network was uniform can be observed in Fig. 3d. Moreover, with the participation of

PDA-prGO and SF, the pore wall thickened and the network structure was changed, which directly improved the mechanical and conductivity properties, meanwhile affecting the swelling rate of hydrogels.

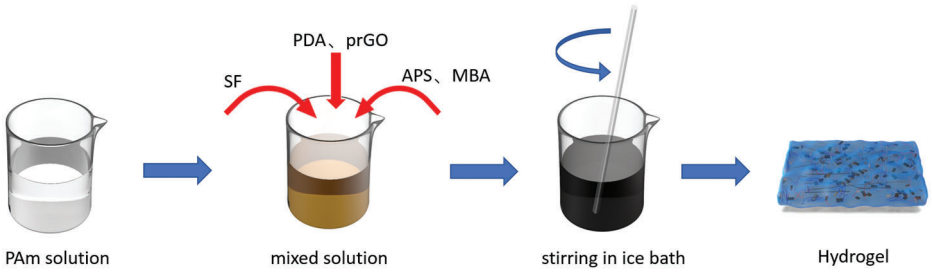

Figure 2: The preparation schematic of the PSPp hydrogel

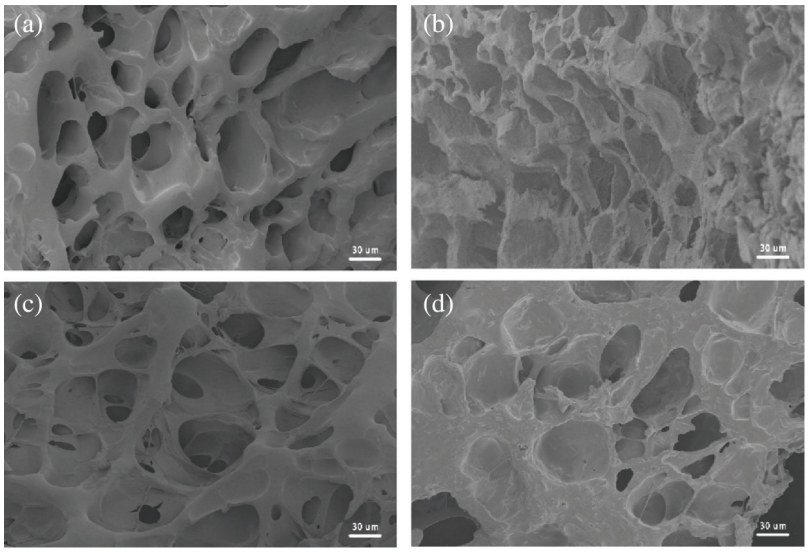

Figure 3: SEM images of (a) PAM; (b) PAM-SF (PS); (c) PAM-PDA-prGO (PPp); (d) PAM-SF-PDA-prGO (PSPp)

The FTIR spectra of PAM, PPp, and PSPp hydrogels can be observed in Fig. 4a. The characteristic absorption peak near 3283 and 3192 cm^{-1} corresponds to the peak of -NH. In the PAM spectrum, the absorption peaks at 2931 and 1447 cm^{-1} correspond to the stretching vibration peaks of -CH_2 and C–N, respectively. These absorption peaks show the typical characteristic of PAM hydrogels. In addition, in the spectrum of PSPp hydrogels, the peak intensity was obviously stronger than other hydrogels after introducing SF. After the formation of hydrogel, the C=O absorption peak moves to 1654 cm^{-1}, which proves that the -$CONH_2$ group is existence in the product [35,36]. Meanwhile, the characteristics peak of symmetric and asymmetric of COO- in the hydrogel can be observed at 1411 and 1616 cm^{-1}, which are significantly weaker than those extracted SF protein (Fig. 4b). Moreover, a new peak at 1268 cm^{-1} can be observed between pure PAM hydrogel and PAM-PDA, which is attributed to the interaction between the -NH_2 group of PAM and the phenolic hydroxyl group of PDA. Meanwhile, the intensity of the adsorption peak of -OH increased, indicating that more hydrogen bonds were formed. Furthermore, the characteristic peak of -NH at 1654 cm^{-1} was shifted to the longer wavenumber region in the spectra of PPp hydrogel, which means the hydrogen bonding interaction exists between GO/prGO and the hydrogel network, and the in-situ polymerization reaction is shown in Figs. 4c and 4d. In addition, GO is involved in the formation of the hydrogel network, which may influence the network structure of hydrogels [37].

To figure out the oxidation effect of DA on GO sheets, the spectra of GO and prGO were analysed and fitted. As shown in Figs. 4c and 4d, at 1067, and 1729 cm^{-1}, corresponds to the C–O bond and the stretching vibration peak of C=O, respectively. In addition, the peak of C–O intensity in rGO is significantly weaker than GO, and the absorption peak of C=O was not clearly observed [38], implying that the oxygen-containing functional group of GO disappears and is partially reduced to rGO. Besides, the presence of GO/prGO mixtures enhanced the conductivity of hydrogels.

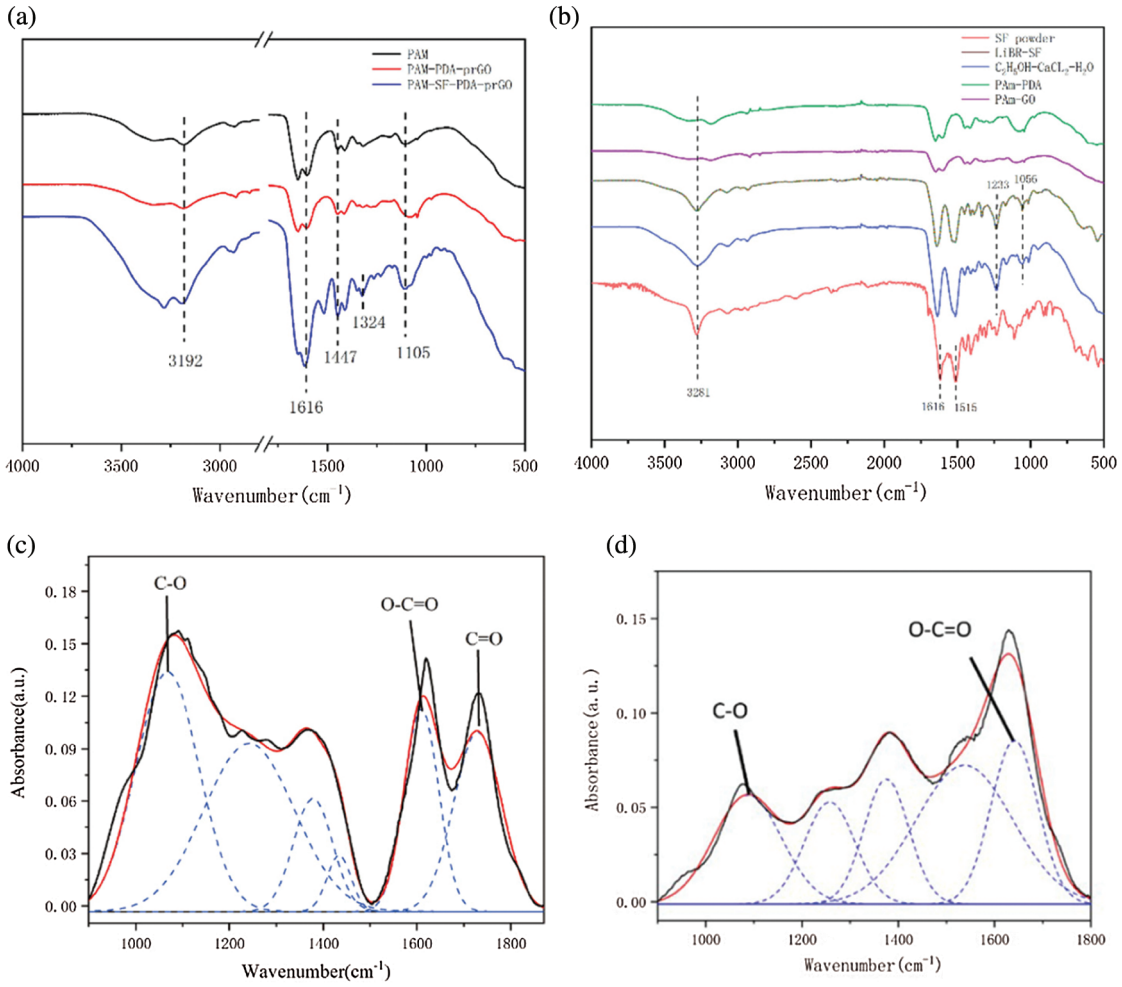

Figure 4: (a–b) FTIR-ATR spectrum of hydrogels, (c–d) FTIR spectrum fitting diagram of GO and prGO in 800–1800 cm^{-1}

The swelling properties of PAM, PS, PSP, and PSPp hydrogels can be observed in Fig. 5a. Those hydrogels exhibited excellent swelling properties. Besides, owing to the hydrophilic groups on the PDA chains, the PAM-PDA hydrogels exhibited stronger swelling properties than pure PAM. In addition, with the same content of PAM and addition of SF, the internal density and porosity of hydrogels were increased effectively, which is one of the reasons for the swelling ratio of PSPp hydrogels being lower than others.

We further tested the mechanical properties of hydrogel with different DA content. The results showed that with the increase of DA content, the hydrogel gradually softened and the stress decreased, shown in Fig. 5b. It is worth noting that when the DA content in the hydrogel is excess 30 mg, the hydrogel is too

soft and difficult to peel from the mold. Therefore, according to the demand for mechanical properties of the hydrogel, 10 mg DA was used in the following experiments.

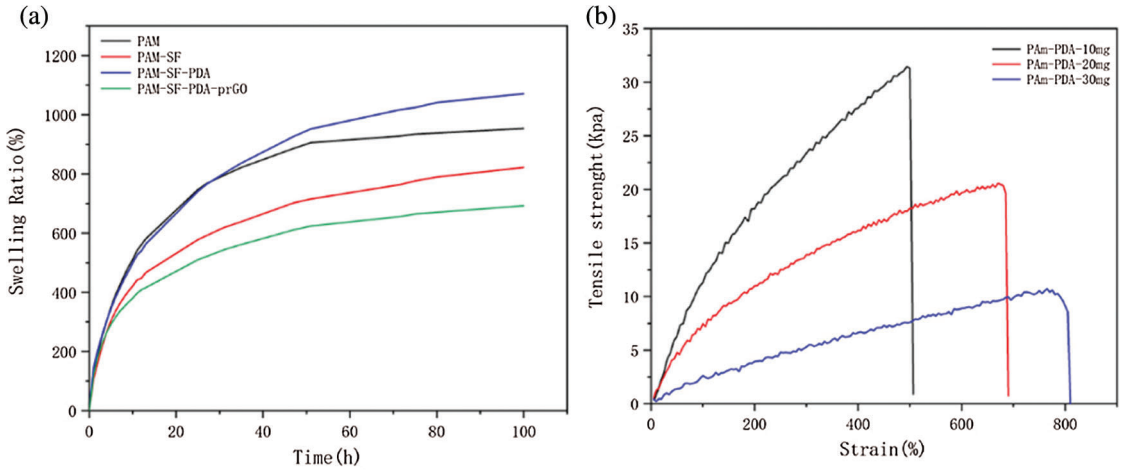

Figure 5: (a) Swelling ratio of hydrogels, (b) Mechanical properties of PAM-PDA hydrogel with different PDA content

The experimental results indicated that the mechanical properties of pure PAM hydrogels could not meet the actual demands. However, with the participation of SF, the mechanical of PS hydrogels can be significantly improved. Fig. 6b demonstrates the results of mechanical tests of PS hydrogels with different SF extraction methods [39,40]. Under the condition of the same SF content, the tensile strength of SF extracted by the ternary solvent is stronger than LiBr, but elongation is weaker. Notably, SF powder-based PS hydrogel with tensile stress of 47.8 KPa, fracture strain of 1350%, mechanical properties are nearly twice than the above two SF-based hydrogels.

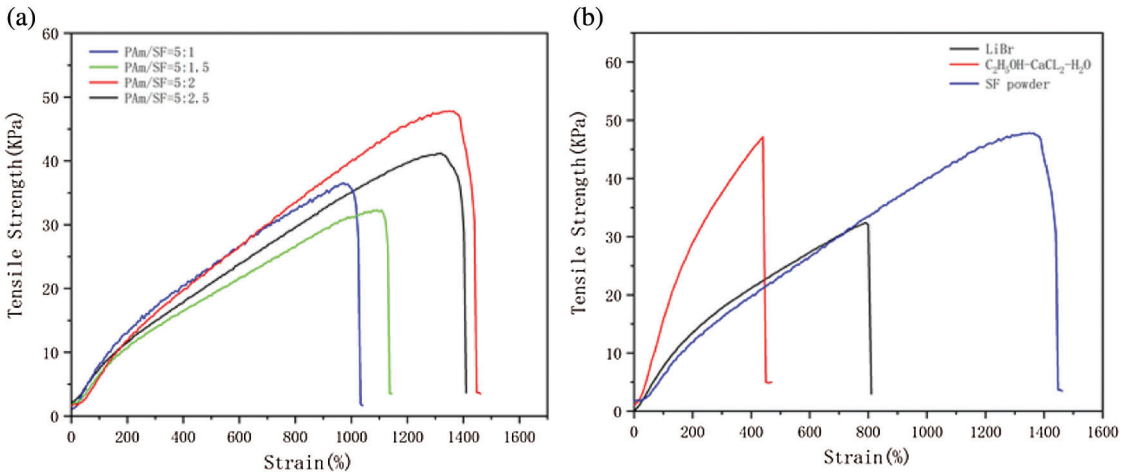

Figure 6: (a) Mechanical properties of PS hydrogels at different ratios, (b) The tensile stress-strain of PS hydrogel prepared from SF extracted by different extraction methods

The above result is due to the stronger degradation of SF heavy chain by ternary solvent than LiBr solution. Therefore, the molecular weight of SF dissolved in the ternary solvent is 64 ± 3 M_w (kDa)[a], which is less than 95 ± 1 M_w (kDa)[a] dissolved in LiBr, implying that the mechanical properties of PS

hydrogels are greatly different due to the SF in different molecular weights. In addition, the molecular weight of silk fibroin powder degummed by high pressure was 250 M_w (kDa)[a], which is much higher than that of SF extracted by LiBr and ternary solvent. Therefore, the PS hydrogel prepared by SF powder exhibits excellent mechanical properties. Moreover, multiple long chains of amino acid and hydroxy are contained in SF, which interact with the functional groups of PAM and PDA chains to form hydrogen bonds, thus enhancing the mechanical properties of PS hydrogels [40].

Furthermore, the hydrogel with the ratio of PAM:SF powder = 5:2 was found to have excellent mechanical properties. Therefore, considering the mechanical properties of the hydrogel, SF powder was used in the following experiments.

The mechanical properties of hydrogels are one of the crucial keys to the fabrication of flexible wearable sensors, therefore, PAM PS PAM-PDA and PSPp hydrogels were compared under the same conditions. All hydrogel samples were cut to the same size and the PAM contents in the hydrogel remained the same. Compared the mechanical properties with pure PAM hydrogel and PAM-SF hydrogel (Fig. 7a), the addition of SF increased the tensile stress ratio by 251%, elongation of 225%, and the measured fracture energy of 421 KJm^{-3} (Eqs. (1) and (2)), W_C is the integral of the stress-strain curve, and T is the converted fracture energy (KJm^{-3}). These results indicated that the participation of the SF endows the PS hydrogels with excellent mechanical properties and which is several times stronger than pure PAM hydrogel. In addition, the PAM-PDA hydrogel exhibited superior elongation of 687% and almost the same tensile stress of 20.3 KPa as PAM. In addition, the PSPp hydrogel had large tensile strength of 60.5 KPa and elongation of 1020%, with fracture energy of 374.86 KJm^{-3}. In addition, hydrogen bonding, van der Waals forces [41], and covalent interactions connect the PAM, SF, and GO channels to each other, which is one of the major reasons for PSPp hydrogels exhibit excellent machinal properties.

$$W_C = \int \sigma d\varepsilon \tag{1}$$

$$T = W_C * 10^{-2} \tag{2}$$

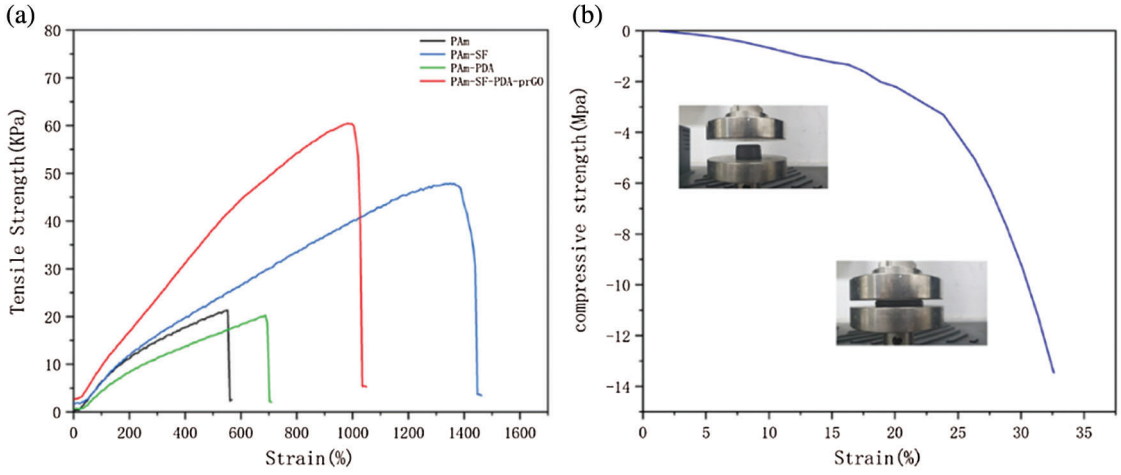

Figure 7: (a) Tensile stress-strain curves of the PAM, PS, PAM-PDA and PSPp hydrogels, (b) compression curves of the PSPp hydrogel

Electrical property is another main factor in evaluating the performance of flexible wearable sensors. The existing GO and DA in the system will have a great influence on the mechanical and electrical properties of the hydrogels. In order to compare the conductivity of hydrogels with different contents of

prGO. It can be observed from Fig. 8a, The content of GO is positively correlated with the conductivity of hydrogel, and the conductivity reached 8.58 mS cm^{-1} at the GO content of 15 mg. When the GO content is between 15 to 20 mg, the conductivity may reach a peak. However, the conductivity of the PAM-PDA-prGO hydrogel begins to decrease when the contents of GO exceed 20 mg. In addition, to explore the effects of different conductive materials on the electrical properties of the hydrogels, MWCNTs were added [42]. As seen in Fig. 8c, the conductivity of CNTs was significantly weaker than prGO. Similarly, the electrical trend of PAM-MWCNTs hydrogel is similar to PAM-PDA-prGO, which indicates that the conductivity of hydrogel will decrease when the concentration of conductive filler reaches the threshold.

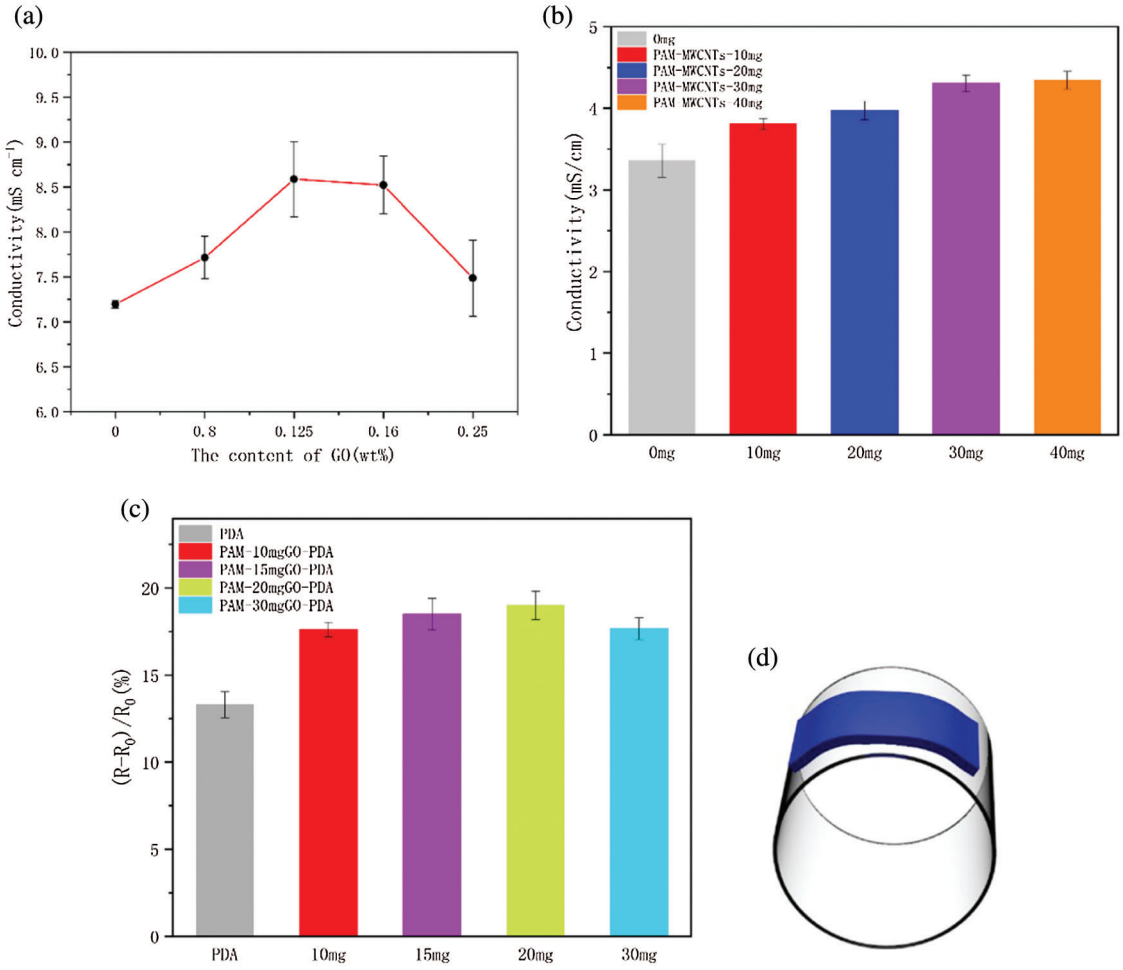

Figure 8: The electrical of the hydrogel. (a) Conductivity of hydrogels with 0, 10, 15, 20, and 30 mg GO. (b) conductivity of PAM-MWCNTs with different contents of CNTs. (c) Sensitive of PAM-PDA-prGO hydrogels with different GO contents. (d) Schematic diagram of sensitivity test

Furthermore, the hydrogels were placed on cylindrical glass (diameter of 6 cm, Fig. 8e) at the same bending curvature to test the deformation sensitivity, Fig. 8d shows the rate of resistance change of hydrogels with different fillers and concentrations ($\Delta R = (R - R_0)/R_0$); R and R_0 are measuring and initial resistance, respectively). The results indicated that the GO addition of 15 and 20 mg in PAM-GO-PDA hydrogel did not change the conductivity of hydrogel significantly. However, after the content of GO in the re1action system reached 30 mg, the conductivity of hydrogels was decreased. The above phenomena indicate that the conductive filler may agglomerate in the cross-linked network after reaching the threshold

value, resulting in a decrease in conductivity and sensitivity. Considering the conductivity, sensitivity and GO dispersion effect. Therefore, PAM-GO (15 mg) was selected in the following experiments.

Figs. 9a and 9b demonstrates the conductivity of pure PAM hydrogel is poor. After adding DA and GO, the conductivity of hydrogel was increased from 3.5 to 9.5 mS cm^{-1}. The excellent conductivity is attributed to the existence of rGO, which is reduced from GO during the self-polymerization process of DA. During this process, oxygen-containing functional groups of GO were decreased and promoted the dispersion of rGO [43]. Therefore, the conductive network was successfully constructed inside the PSPp hydrogels and sharply improved the conductivity to10.5 mS cm^{-1}. Furthermore, with the participation of DA and GO, the conductivity of the hydrogels was increased from 3.5 to 9.5 mS cm^{-1}, and ΔR reached 20.9%, indicating that the hydrogel has excellent conductivity and is sensitive to small deformation, which provided the foundation for flexible wearable sensors. Fig. 9c shows the stretch and recovery response times of the PSPp sensor are less than 300 ms. In addition, under the elongation of 200%, the cyclic tensile test of PSPp sensor was carried out 3485 times (50 cycles). Fig. 9d revealed that there is almost no significant difference between each cycle, considering that the PSPp hydrogel sensor has good stability.

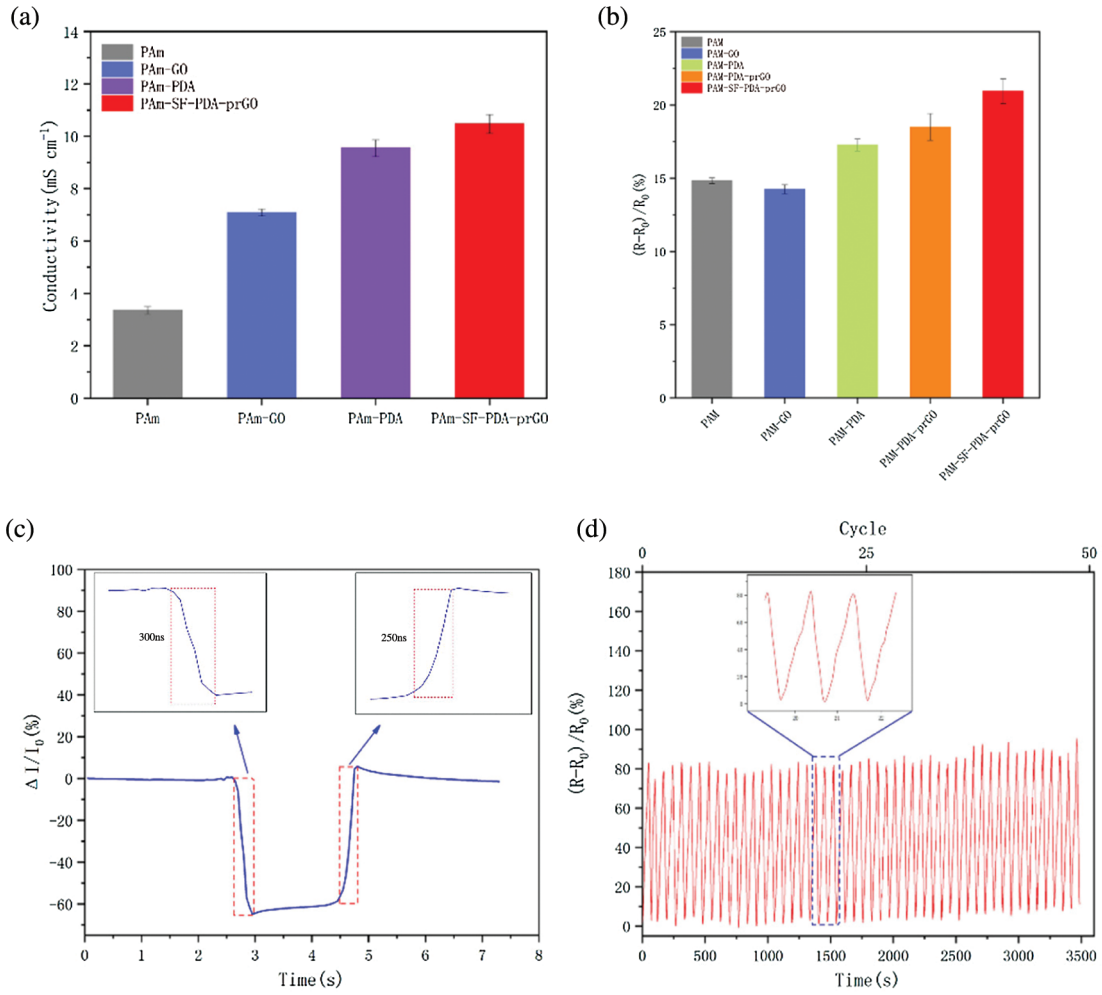

Figure 9: (a) Conductivity of the PAM, PS, PAM-PDA and PSPp hydrogels, (b) the sensing response of PAM, PAM-GO, PS, PAM-PDA and PSPp hydrogels, (c) sensor response time to stretch-recovery, (d) anti-fatigue test of PSPp sensor for 3485 times

Self-adhesion is one of the characteristics of flexible wearable sensors, which greatly improves the convenience of the sensors. Subsequently, the adhesive strength property of hydrogel was investigated. Fig. 10a shows the adhesion of PAM hydrogel, reaching 18.5 KPa, and PSPp hydrogel reaching 21.96 KPa. The above adhesion ability is owing to the catechol group of the PDA chains. Free phenol hydrogel interacts with -NH_2 groups, -SH groups on skin and cation-π, π–π interaction formed between the catechol groups and the contact surfaces are led to the hydrogels to adhere to almost all surfaces, such as glass, rubber, and skin (Figs. 10b–10d).

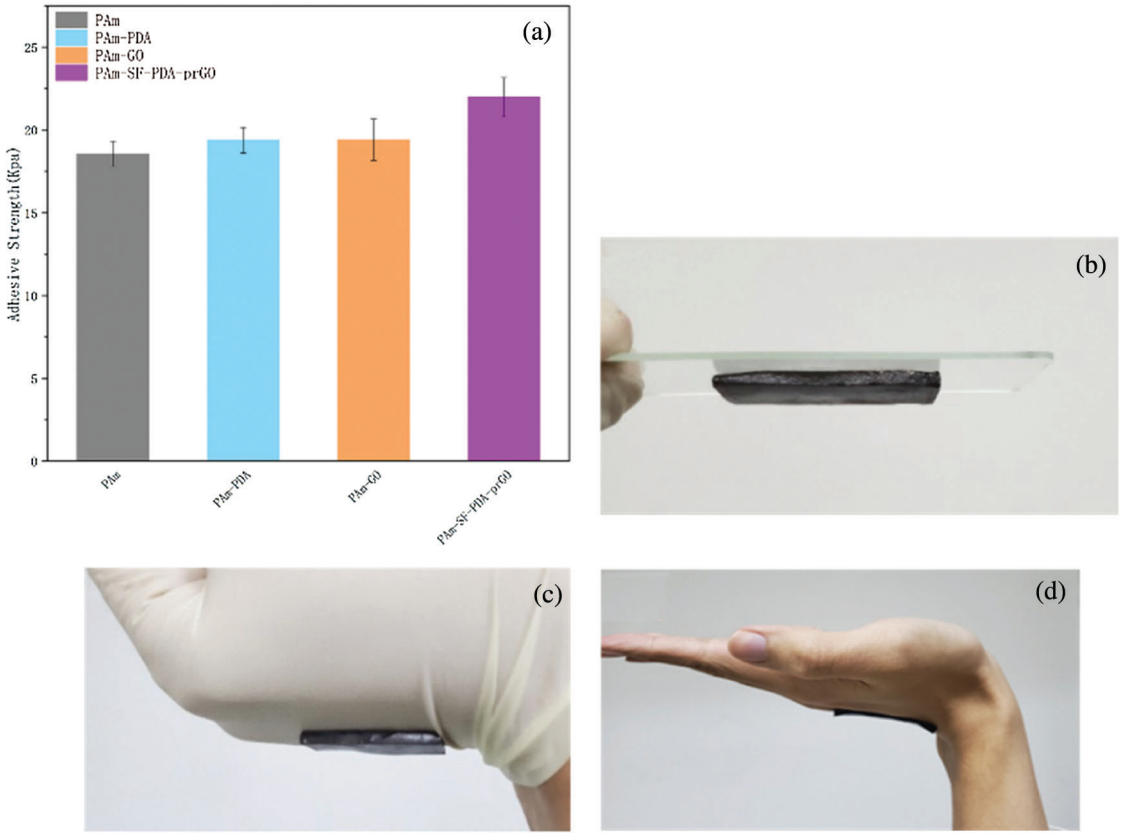

Figure 10: (a) The adhesive strength of the PAM, PAM-PDA and PSPp hydrogels, (b–d) the PSPp hydrogels stably adhered to glass, rubber, and skin surfaces

Notably, the PSPp hydrogel exhibits high sensitivity and wide applications in human motion monitoring. Therefore, PSPp hydrogels can be mounted as flexible wearable devices to monitor a series of human motions in real-time. As shown in Fig. 11, connect the sensor to the electrochemical workstation through wires to monitor the signals generated by the movement of different parts of our body. In addition, the different joint motions [44], such as finger, wrist, and knee (Figs. 12a–12c) can be identified through resistance changes of the hydrogel sensor. In particular, the sensor can identify different bending angels of neck. For instance, as the volunteer flexed and extended their joints repetitively, the sensor can record the complete activity process through the change of resistance and the curve shows a stable response peak and valley. In addition, the resistance curve is positively correlated with the degree of motion deformation. Moreover, the joint motion of the finger shows a higher peak than the leg and wrist, which is because the finger moving range larger than the leg.

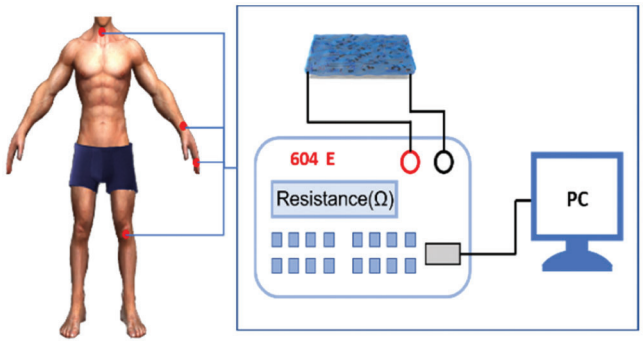

Figure 11: Schematic diagram of human motion detection by PSPp hydrogel sensor

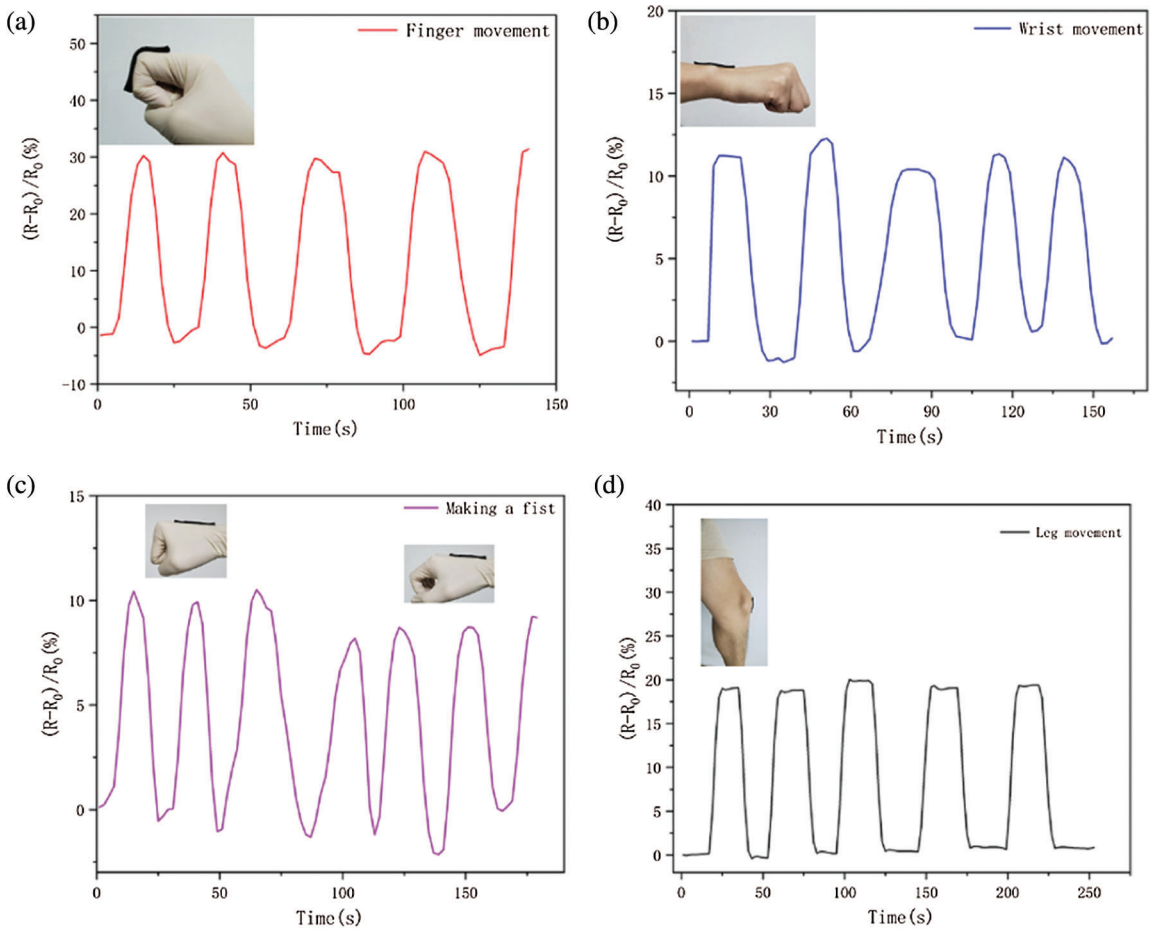

Figure 12: (Continued)

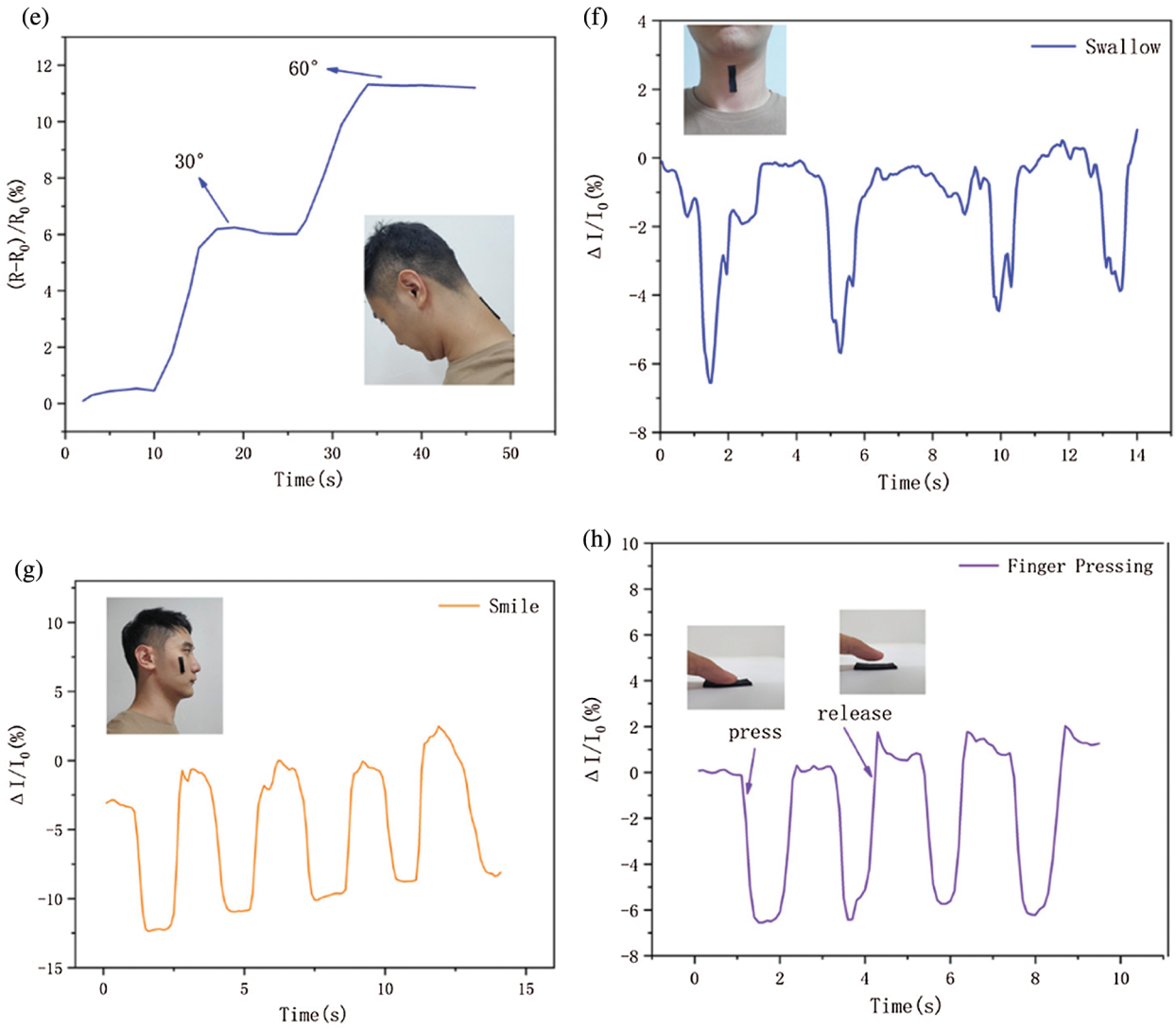

Figure 12: PSPp sensors used to monitor physical motions. (a–e) Human activity detection, such as the finger, wrist, make a fist, leg, and neck. (f–h) Relative current variations of swallow, smile, and finger pressing

In addition, due to the high sensitivity of the PSPp sensor, it can respond to different deformations of the hand include loose fist and tight fist, as shown in Fig. 12d. Meanwhile, the sensor can also detect large-scale motion of leg flexion and extension. Interestingly, When the neck is bent at different angles (such as 0°, 30°, and 60°) and maintained for several seconds, the PSPp sensor can stably respond to different states.

Moreover, the PSPp sensor is also can be used to monitor tiny changes in the face, the PSPp sensor was mounted on the face and throat to detect some small-scale signals such as smile and swallow (Figs. 12f–12g). The same change trend can be observed with the same expression, implying that the PSPp sensor is able to detect tiny motion. Additionally, the PSPp sensor also exhibits high sensitivity to pressure signals, as can be observed in Fig. 12h. Therefore, the sensor can detect regular motion with large-scale and small-scale accuracy and exhibits great stability.

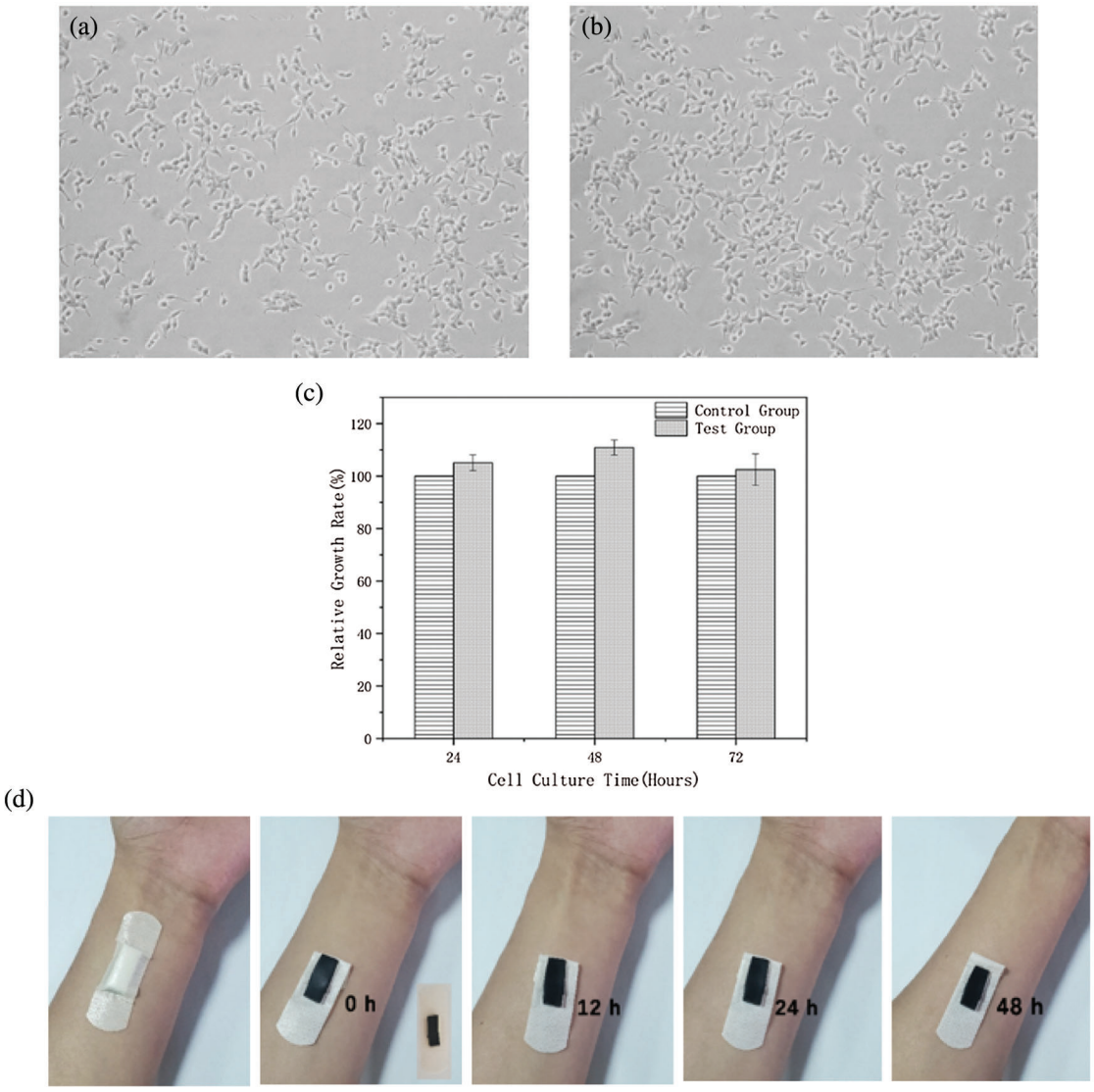

Figure 13: Biocompatibility test. (a) 48 h cell morphology of control group (b) test group (c) Relative cell growth rate for 24, 48, and 72 h (d) Wear the hydrogel sensor for 48 h

The biocompatibility of PSPp hydrogel was evaluated by in vitro cytotoxicity test (CCK-8 method). Fig. 13c shows the cell proliferation rate of NIH3T3 fibroblasts cultured for 24, 48 and 72 h, and the quantitative proliferation rate of fibroblasts reached the peak after 48 h. It can be observed from the figure that the relative growth rate of the test group was not affected, indicating that the hydrogel had no negative effect on cell growth. In addition, as shown in Figs. 13a and 13b, there was no significant difference in cell morphology of the test group. Meanwhile, NIH3T3 fibroblasts were irregularly fusiform and grew normally after culture. In particular, the PSPp hydrogel adheres to the arm for 48 h without any allergic reaction observed (Fig. 13d). Therefore, the hydrogel sensor exhibits excellent biocompatibility and can be used as a wearable medical device and a portable real-time health monitoring for direct contact.

Furthermore, the 3-channel with 5-electrode ECG detection equipment was used to acquisitive human ECG signals under the same experimental conditions (Fig. 14c). The PSPp hydrogel was encapsulated as an electrode to replace the commercial electrode to detect the ECG signals of the human body. The results indicate that there was almost no significant difference compared with commercial electrodes (Figs. 14a and 14b). Besides, owing to the excellent conductivity, the PSPp hydrogel is more luminous than the pure PAM hydrogel when it connects with an LED lamp (Figs. 14d and 14e). Therefore, the PAM-SF-PDA-prGO hydrogel can detect small physiological signals and has good biocompatibility with the skin and cells, revealing its broad application prospects in the field of flexible wearable devices.

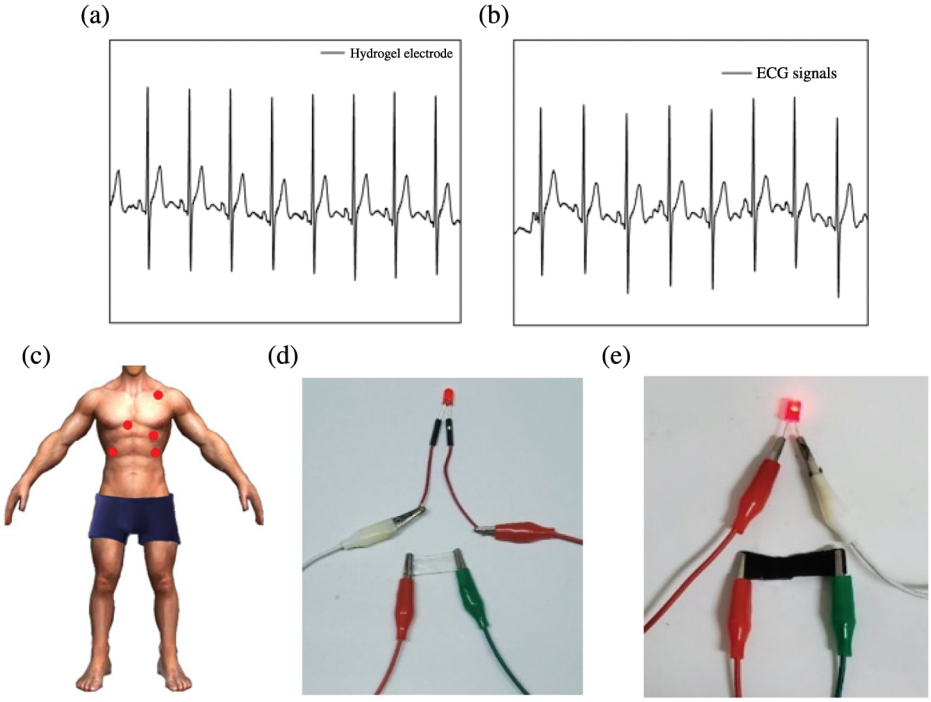

Figure 14: (a–b) Detection of human ECG. (c) Schematic diagram of ECG measurement. (d–e) Digital photographs of PAM and PSPp sensors lighting up the red LED lamp

4 Conclusion

In summary, the PSPp hydrogel flexible sensor with excellent mechanical and electrical properties was designed and fabricated by rationally integrating polymer of PAM, SF, PDA and GO. The PSPp sensor exhibited high tensile strength of 60.5 KPa, elongation of 1020%, fast response and it is also sensitive to sensing strain/pressure signals. Moreover, the rGO in the system is the key factor for the excellent conductivity and sensitivity of the hydrogels. Remarkably, the hydrogel sensor can efficiently monitor include large-scale and small-scale motions (joints, smile, swallow and press, etc.), which provided the foundation of flexible wearable sensors for post-healing, healthcare, and real-time monitoring. Moreover, the PSPp hydrogel exhibits excellent biocompatibility and could be used as an electrode to detect ECG signals. Therefore, the PSPp hydrogel as a multifunctional material is one of the candidates for flexible wearable devices, which is expected to realize long-term and real-time monitoring in many fields, such as human motion and physiological signals.

Funding Statement: Smart Medicine Research Project of Chongqing Medical University in 2020 (YJSZHYX202022); Smart Medicine Research Project of Chongqing Medical University (ZHYX2019019); Chongqing Research Program of Basic Research and Frontier Technology (cstc2018jcyjAX0165).

Conflicts of Interest: The authors declare that they have no conflicts of interest to report regarding the present study.

References

1. Bai, J. H., Ran, W., Ju, M. X., Zhou, J. X., Zhang, L. X. et al. (2020). Facile preparation and high performance of wearable strain sensors based on ionically cross-linked composite hydrogels. *Science China Materials, 64(4),* 942–952. DOI 10.1007/s40843-020-1507-0.
2. Chang, X. H., Chen, L. R., Chen, J. W., Zhu, Y. T., Guo, Z. H. (2021). Advances in transparent and stretchable strain sensors. *Advanced Composites and Hybrid Materials, 4(3),* 435–450. DOI 10.1007/s42114-021-00292-3.
3. Lv, J., Kong, C., Yang, C., Yin, L., Jeerapan, I. et al. (2019). Wearable, stable, highly sensitive hydrogel-graphene strain sensors. *Beilstein Journal of Nanotechnology, 10(1),* 475–480. DOI 10.3762/bjnano.10.47.
4. Zhang, Y. F., Gong, M., Wan, P. B. (2021). MXene hydrogel for wearable electronics. *Matter, 4(8),* 2655–2658. DOI 10.1016/j.matt.2021.06.041.
5. Jia, Y. P., Pan, Y. M., Wang, C. F., Liu, C. T., Shen, C. Y. et al. (2021). Flexible Ag microparticle/MXene-based film for energy harvesting. *Nano-Micro Letters, 13(1),* 201. DOI 10.1007/s40820-021-00729-w.
6. Wan, D., Yang, J., Cui, X. J., Ma, N. C., Wang, Z. S. et al. (2021). Human body-based self-powered wearable electronics for promoting wound healing driven by biomechanical motions. *Nano Energy, 89,* 106465. DOI 10.1016/j.nanoen.2021.106465.
7. Li, M. M., Chen, X., Li, X. T., Dong, J., Zhao, X. et al. (2021). Wearable and robust polyimide hydrogel fiber textiles for strain sensors. *ACS Applied Materials & Interfaces, 13(36),* 43323–43332. DOI 10.1021/acsami.1c10055.
8. Yao, F., Zhang, D. Y., Zhang, C. H., Yang, W. T., Deng, J. P. (2013). Preparation and application of abietic acid-derived optically active helical polymers and their chiral hydrogels. *Bioresource Technology, 129,* 58–64. DOI 10.1016/j.biortech.2012.10.157.
9. Zhao, Z. Y., Wang, H. N., Huang, H. B., Li, L., Yu, X. H. (2021). Graphene oxide/polypyrrole/polyaniline composite hydrogel synthesized by vapor-liquid interfacial method for supercapacitors. *Colloids and Surfaces A: Physicochemical and Engineering Aspects, 626,* 127125. DOI 10.1016/j.colsurfa.2021.127125.
10. Spencer, A. R., Primbetova, A., Koppes, A. N., Koppes, R. A., Fenniri, H. et al. (2018). Electroconductive gelatin methacryloyl-PEDOT:PSS composite hydrogels: Design, synthesis, and properties. *ACS Biomaterials Science & Engineering, 4(5),* 1558–1567. DOI 10.1021/acsbiomaterials.8b00135.
11. Jeong, J., Park, J., Kim, Y., Yang, S., Jeong, S. et al. (2020). Gamma ray-induced polymerization and cross-linking for optimization of PPy/PVP hydrogel as biomaterial. *Polymers, 12(1),* 111. DOI 10.3390/polym12010111.
12. Han, L., Yan, L. W., Wang, M. H., Wang, K. F., Fang, L. M. et al. (2018). Transparent, adhesive, and conductive hydrogel for soft bioelectronics based on light-transmitting polydopamine-doped polypyrrole nanofibrils. *Chemistry of Materials, 30(16),* 5561–5572. DOI 10.1021/acs.chemmater.8b01446.
13. Yan, T., Wang, Z., Pan, Z. (2018). Flexible strain sensors fabricated using carbon-based nanomaterials: A review. *Current Opinion in Solid State and Materials Science, 22(6),* 213–228. DOI 10.1016/j.cossms.2018.11.001.
14. Gu, Y. D., Zhang, T., Chen, H., Wang, F., Pu, Y. M. et al. (2019). Mini review on flexible and wearable electronics for monitoring human health information. *Nanoscale Research Letters, 14(1),* 263. DOI 10.1186/s11671-019-3084-x.
15. Pang, Y., Yang, Z., Yang, Y., Ren, T. L. (2020). Wearable electronics based on 2D materials for human physiological information detection. *Small, 16(15),* 1901124. DOI 10.1002/smll.201901124.
16. Kim, J., Campbell, A. S., de Ávila, B. E., Wang, J. (2019). Wearable biosensors for healthcare monitoring. *Nature Biotechnology, 37(4),* 389–406. DOI 10.1038/s41587-019-0045-y.

17. Han, Z. Y., Cheng, Z. Q., Chen, Y., Li, B., Liang, Z. W. et al. (2019). Fabrication of highly pressure-sensitive, hydrophobic, and flexible 3D carbon nanofiber networks by electrospinning for human physiological signal monitoring. *Nanoscale, 11(13),* 5942–5950. DOI 10.1039/C8NR08341J.
18. Sun, J. C., Shakya, S., Gong, M., Liu, G. M., Wu, S. et al. (2019). Combined application of graphene-family materials and silk fibroin in biomedicine. *ChemistrySelect, 4(19),* 5745–5754. DOI 10.1002/slct.201804034.
19. Fan, S. N., Zhang, Y., Huang, X. Y., Geng, L. H., Shao, H. L. et al. (2019). Silk materials for medical, electronic and optical applications. *Science China Technological Sciences, 62(6),* 903–918. DOI 10.1007/s11431-018-9403-8.
20. Qi, Y., Wang, H., Wei, K., Yang, Y., Zheng, R. et al. (2017). A review of structure construction of silk fibroin biomaterials from single structures to multi-level structures. *International Journal of Molecular Sciences, 18(3),* 237. DOI 10.3390/ijms18030237.
21. Liao, M., Wan, P., Wen, J., Gong, M., Wu, X. et al. (2017). Wearable, healable, and adhesive epidermal sensors assembled from mussel-inspired conductive hybrid hydrogel framework. *Advanced Functional Materials, 27(48),* 1703852. DOI 10.1002/adfm.201703852.
22. Annabi, N., Shin, S. R., Tamayol, A., Miscuglio, M., Bakooshli, M. A. et al. (2016). Highly elastic and conductive human-based protein hybrid hydrogels. *Advanced Materials, 28(1),* 40–49. DOI 10.1002/adma.201503255.
23. He, F. L., You, X. Y., Gong, H., Yang, Y., Bai, T. et al. (2020). Stretchable, biocompatible, and multifunctional silk fibroin-based hydrogels toward wearable strain/pressure sensors and triboelectric nanogenerators. *ACS Applied Materials & Interfaces, 12(5),* 6442–6450. DOI 10.1021/acsami.9b19721.
24. Khan, M., Shah, L. A., Khan, M. A., Khattak, N. S., Zhao, H. B. (2020). Synthesis of an un-modified gum arabic and acrylic acid based physically cross-linked hydrogels with high mechanical, self-sustainable and self-healable performance. *Materials Science and Engineering: C, 116,* 111278. DOI 10.1016/j.msec.2020.111278.
25. Oral, C. B., Yetiskin, B., Okay, O. (2020). Stretchable silk fibroin hydrogels. *International Journal of Biological Macromolecules, 161,* 1371–1380. DOI 10.1016/j.ijbiomac.2020.08.040.
26. Ming, J. F., Pan, F. K., Zuo, B. Q. (2015). Structure and properties of protein-based fibrous hydrogels derived from silk fibroin and sodium alginate. *Journal of Sol-Gel Science and Technology, 74(3),* 774–782. DOI 10.1007/s10971-015-3662-z.
27. Liu, S. J., Qiu, Y., Yu, W., Zhang, H. B. (2020). Highly stretchable and self-healing strain sensor based on gellan gum hybrid hydrogel for human motion monitoring. *ACS Applied Polymer Materials, 2(3),* 1325–1334. DOI 10.1021/acsapm.9b01200.
28. Khan, M., Shah, L. A., Rehman, T., Khan, A., Iqbal, A. et al. (2020). Synthesis of physically cross-linked gum arabic-based polymer hydrogels with enhanced mechanical, load bearing and shape memory behavior. *Iranian Polymer Journal, 29(4),* 351–360. DOI 10.1007/s13726-020-00801-z.
29. Hao, S. W., Shao, C. Y., Meng, L., Cui, C., Xu, F. et al. (2020). Tannic acid–silver dual catalysis induced rapid polymerization of conductive hydrogel sensors with excellent stretchability, self-adhesion, and strain-sensitivity properties. *ACS Applied Materials & Interfaces, 12(50),* 56509–56521. DOI 10.1021/acsami.0c18250.
30. Wang, Y. L., Huang, H. L., Wu, J. L., Han, L., Yang, Z. L. et al. (2020). Ultrafast self-healing, reusable, and conductive polysaccharide-based hydrogels for sensitive ionic sensors. *ACS Sustainable Chemistry & Engineering, 8(50),* 18506–18518. DOI 10.1021/acssuschemeng.0c06258.
31. Yang, X., Niu, X. H., Mo, Z. L., Guo, R. B., Liu, N. J. et al. (2019). Electrochemical chiral interface based on the michael addition/schiff base reaction of polydopamine functionalized reduced graphene oxide. *Electrochimica Acta, 319,* 705–715. DOI 10.1016/j.electacta.2019.07.040.
32. Jing, X., Mi, H. Y., Lin, Y. J., Enriquez, E., Peng, X. F. et al. (2018). Highly stretchable and biocompatible strain sensors based on mussel-inspired super-adhesive self-healing hydrogels for human motion monitoring. *ACS Applied Materials & Interfaces, 10(24),* 20897–20909. DOI 10.1021/acsami.8b06475.
33. Kou, Y. J., Zhou, W. Y., Xu, L., Cai, H. W., Wang, G. H. et al. (2019). Surface modification of GO by PDA for dielectric material with well-suppressed dielectric loss. *High Performance Polymers, 31(9–10),* 1183–1194. DOI 10.1177/0954008319837744.

34. Hou, C., Xu, Z. J., Qiu, W., Wu, R. H., Wang, Y. N. et al. (2019). A biodegradable and stretchable protein-based sensor as artificial electronic skin for human motion detection. *Small, 15(11),* 1805084. DOI 10.1002/smll.201805084.
35. Wu, G. Z., Mahyar, P. S., Xiao, X. L., Ding, F. C., Ke, D. et al. (2021). Fabrication of capacitive pressure sensor with extraordinary sensitivity and wide sensing range using PAM/BIS/GO nanocomposite hydrogel and conductive fabric. *Composites Part A: Applied Science and Manufacturing, 145,* 106373. DOI 10.1016/j.compositesa.2021.106373.
36. Wang, C., Du, Y. L., Chen, B. Y., Chen, S. J., Wang, Y. P. (2019). A novel highly stretchable, adhesive and self-healing silk fibroin powder-based hydrogel containing dual-network structure. *Materials Letters, 252,* 126–129. DOI 10.1016/j.matlet.2019.05.129.
37. Zhang, L. Q., Jiang, Q. F., Zhao, Y. M., Yuan, J., Zha, X. Y. et al. (2022). Strong and tough PAm/SA hydrogel with highly strain sensitivity. *Journal of Renewable Materials, 10(2),* 415–430. DOI 10.32604/jrm.2022.016650.
38. Zhang, Y., Liang, B., Jiang, Q. F., Li, Y., Feng, Y. et al. (2020). Flexible and wearable sensor based on graphene nanocomposite hydrogels. *Smart Materials and Structures, 29(7),* 75027. DOI 10.1088/1361-665X/ab89ff.
39. Kim, H. J., Yang, Y. J., Oh, H. J., Kimura, S., Wada, M. et al. (2017). Cellulose–silk fibroin hydrogels prepared in a lithium bromide aqueous solution. *Cellulose, 24(11),* 5079–5088. DOI 10.1007/s10570-017-1491-7.
40. Wang, Q., Chen, Q., Yang, Y. H., Shao, Z. Z. (2013). Effect of various dissolution systems on the molecular weight of regenerated silk fibroin. *Biomacromolecules, 14(1),* 285–289. DOI 10.1021/bm301741q.
41. Wang, X., Wang, Y., Zhao, N., Zheng, M., Guo, Y. et al. (2021). Van der Waals enhanced interfacial interaction in cellulose/zinc oxide nanocomposite coupled by graphitic carbon nitride. *Carbohydrate Polymers, 268,* 118235. DOI 10.1016/j.carbpol.2021.118235.
42. Zhou, J., Zhao, Z. Y., Hu, R. M., Yang, J. L., Xiao, H. et al. (2020). Multi-walled carbon nanotubes functionalized silk fabrics for mechanical sensors and heating materials. *Materials & Design, 191,* 108636. DOI 10.1016/j.matdes.2020.108636.
43. Cheng, D. S., Bai, X., Pan, J. J., Ran, J. H., Wu, J. H. et al. (2019). Immobilizing reduced graphene oxide on polydopamine-templated PET fabrics for UV protection, electrical conduction and application as wearable sensors. *Materials Chemistry and Physics, 241,* 122371. DOI 10.1016/j.matchemphys.2019.122371.
44. Jin, R., Xu, J. J., Duan, L. J., Gao, G. H. (2021). Chitosan-driven skin-attachable hydrogel sensors toward human motion and physiological signal monitoring. *Carbohydrate Polymers, 268,* 118240. DOI 10.1016/j.carbpol.2021.118240.